

Publicising Lattice Field Theory through Visualisation

**James Biddle, Josh Charvetto, Waseem Kamleh, Derek Leinweber*, Helen Piercy,
Ethan Puckridge, Finn Stokes, Ross D. Young*, James Zanotti†**

*Centre for the Subatomic Structure of Matter, Department of Physics,
The University of Adelaide, SA 5005, Australia*

E-mail: derek.leinweber@adelaide.edu.au

The gluon field configurations that form the foundation of every lattice QCD calculation contain a rich diversity of emergent nonperturbative structure. Visualisations of these phenomena not only serve to explain the concept of a nontrivial vacuum but also entertain a diverse audience from research funding panels to the next generation of science enthusiasts. In this brief review, a collection of QCD-vacuum visualisations is presented including the structure of chromo-electromagnetic fields, centre-cluster evolution at finite temperature, the structure of projected centre vortices, and novel correlations between the electromagnetic fields of QED and the chromo-electromagnetic fields of QCD in QED+QCD dynamical-fermion simulations from the QCDSF collaboration.

*The 36th Annual International Symposium on Lattice Field Theory - LATTICE2018
22-28 July, 2018
Michigan State University, East Lansing, Michigan, USA.*

*Speaker.

†This research is supported with supercomputing resources provided by the Phoenix HPC service at the University of Adelaide and the National Computational Infrastructure (NCI) supported by the Australian Government. This research is supported by the Australian Research Council through Grants No. DP140103067, DP150103164, and LE160100051.

1. Understanding Complexity through Visualisation

Deep insight into the mechanisms giving rise to quantum phenomena can be obtained through the visualisation of the complex scientific data sets considered in theoretical computational-physics calculations. These are insights that would otherwise remain hidden in the typical gigabyte data sets of modern quantum field theory. If one can see what's going on, it is easy to share this new understanding with a broad audience. In this sense, a picture is worth a thousand equations.

For 20 years, the Centre for the Subatomic Structure of Matter (CSSM) has aimed to reveal the quantum phenomena of the nontrivial vacuum that underpins every calculation in lattice QCD. The focus is on displaying the results of genuine calculations and creating new insights into the fundamental mechanisms that give rise to the observed phenomena. Visualisations of these phenomena not only serve to explain the novel concept of a nontrivial vacuum but also inform and entertain a diverse audience from researchers in the field to the next generation of science enthusiasts.

These data sets contain a rich diversity of emergent structure and a variety of approaches to revealing this structure has been explored. In this presentation, four approaches to understanding QCD vacuum structure are presented. Each approach is illustrated by animations which are available via YouTube, enabling easy dissemination through social media. The original HD-streaming format videos have also been placed on line. In the following, references contain active URL's to these animations.

2. Structure of the QCD Vacuum

Among the earliest of CSSM visualisations are animations of the Euclidean action density and the topological charge density of gluon field configurations [1]. Calculations were based on pure SU(3) gluon dynamics with the standard Wilson action at $\beta = 6.0$ on a $24^3 \times 36$ lattice. The first coordinate was used for the time axis creating a $24^2 \times 36$ spatial volume with a lattice spacing of 0.1 fm. It is these calculations that captured the attention of Prof Frank Wilczek as he prepared his 2004 Nobel Prize lecture. Ref. [2] provides a link to the *QCD Lava Lamp* animation that appeared in his Nobel Lecture [3]. In support of the Nobel Lecture a web page incorporating the best algorithms and visualisation techniques of the time was created to engage the public's interest [4]. Since then these images and animations have appeared in popular-science publications, YouTube channels [5, 6], public talks and lectures, conference presentations, journal articles, annual reports, grant applications, school visits [7] and newspaper articles.

In this report, a new animation [8] is presented drawing on the legacy calculations of the Nobel Lecture and providing new insights into the structure of the eight chromo-electric and eight chromo-magnetic fields. Correlations between the energy density, topological charge density and the 16 vector fields are explored. The HD-streaming version is available via the link in Ref. [9].

Calculations of the chromo-electromagnetic fields proceed via the $\mathcal{O}(a^4)$ -five-loop improved field-strength tensor, $F_{\mu\nu}$, designed to ensure the most local 1×1 and 1×2 clover terms make up 96% of the loop contributions [10]. To explore the long-distance nonperturbative phenomena of the vacuum, short-distance fluctuations are suppressed via 25 sweeps of cooling with the mean-field-improved $\mathcal{O}(a^4)$ -three-loop improved action [11], ensuring the lattice operators are accurate while preserving topological structure within the gauge fields. After assigning the electric and magnetic

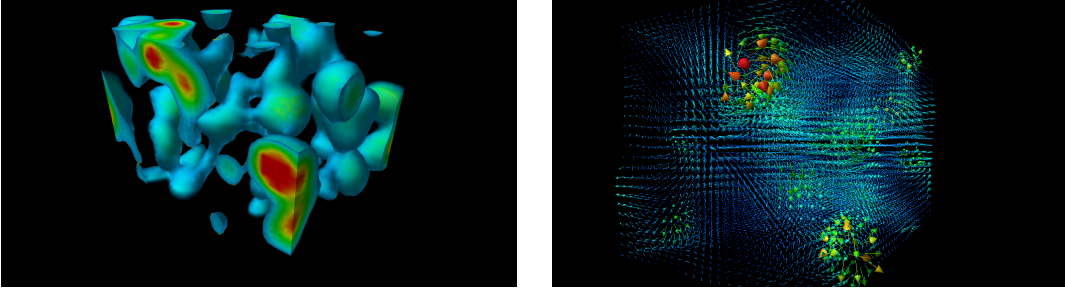


Figure 1: Frames from the animation of Refs. [8, 9] illustrating the energy density (left) and one of the chromo-magnetic fields composing the nontrivial QCD vacuum.

fields in the Euclidean field-strength tensor for the case with the first coordinate playing the role of time, the eight fields are extracted via a trace with the Gell-Mann matrices.

The associated animation [8, 9], illustrates the reduction of the energy density of the gluon field in the first 25 frames of the animation and then displays the time dependence over the 24 frames of the periodic lattice. Areas of high energy density are rendered in red and regions of moderate energy density are rendered in blue. Low-energy regions are not rendered so we can see into the volume. Subsequently, the eight chromo-electric and eight chromo-magnetic gluon fields giving rise to the energy density are illustrated in Landau gauge [12]. Here the colour and length of the arrows describe the magnitude of the vector fields. Figure 1 displays two frames from the animation. Finally, the animation presents correlations with the topological charge density with regions of positive density rendered in red through yellow and regions of negative density rendered blue through cyan.

3. Visualisation of Centre Clusters in Local Polyakov Loops

In Ref. [13] an anisotropic gauge action was used to explore the evolution of coherent centre domains in the gluon field under both temperature and the Hybrid Monte Carlo (HMC) update algorithm. Centre clusters are defined in terms of the complex-valued local Polyakov loop whose expectation value acts as an order parameter for the finite temperature phase transition in QCD. It has an expectation value of zero in the confined phase and a nonzero expectation value in the deconfined phase [14]. The local Polyakov loop is defined as

$$L(\vec{x}) := \text{Tr} \left(\mathcal{P} \exp \left[ig \int dx^0 A_0(x) \right] \right) = \text{Tr} \prod_{t=1}^{N_t} U_0(t, \vec{x}) = \rho(\vec{x}) e^{i\phi(\vec{x})},$$

where it is decomposed into a phase, $\phi(\vec{x})$ and a magnitude, $\rho(\vec{x})$ in the final expression. Both the proximity of the phase to one of the cube-roots of one and the magnitude are considered in visualising the structure of the centre domains of the gluon field. In either case, the most proximal cube root of one to the phase is indicated by the use of colour.

To investigate the larger-scale behaviour of the clusters, small scale noise is removed from the visualisation by performing four sweeps of stout-link smearing prior to calculating the Polyakov loops. Fig. 2 illustrates two different ways of defining the clusters. In Fig. 2b, clusters are rendered where the phase $\phi(\vec{x})$ is within some small window around each centre phase, and the rest of the volume is rendered transparent. The evolution of these clusters with HMC simulation time is

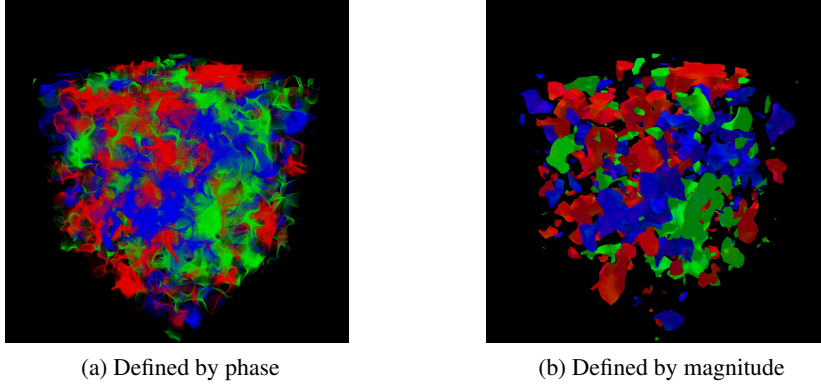


Figure 2: Centre clusters on a gauge field configuration at $T = 0.89(1) T_C$. Similar structure is revealed for centre clusters defined as regions proximal to a single centre phase, and as regions with a larger magnitude. Four sweeps of stout-link smearing are applied to the gauge links prior to calculating the Polyakov loops. The length of each side of the cubic volume is 2.4 fm.

presented in Refs. [15, 16], showing how centre clusters are slowly moving. The animation [15, 16] reveals correlations in the centre clusters persisting for approximately 5 seconds corresponding to 25 HMC trajectories. The temperature dependence of the centre-cluster structure is also explored in these animations where a single phase eventually dominates above the critical temperature. In Fig. 2b, and the animation of Ref. [17, 18], the clusters are rendered where the magnitude $\rho(\vec{x})$ is above some threshold.

These fundamental structures support the concept of hadrons being described as a quark core dressed by a meson cloud. Within these coherent centre domains, colour-singlet quark-antiquark pairs or three-quark triplets have a finite energy and are spatially correlated. Thus, these fundamental domains govern the size of the quark cores of hadrons. As one domain dominates the vacuum above the critical temperature, the correlation length diverges and quarks become deconfined.

4. Structure of Projected Centre Vortices in the Nontrivial QCD Vacuum

Recent research is now exposing the centre-vortex structure of nonperturbative gluon-field configurations to be the most fundamental aspect of nonperturbative vacuum structure giving rise to both confinement and dynamical chiral-symmetry breaking. Removal of SU(3) centre vortices removes confinement, while consideration of the vortices alone provides confinement [19]. Similarly, removal of vortices suppresses the infrared enhancement of the gluon propagator, while consideration of the vortices alone provides the well-known infrared enhancement [20]. Studies of the nonperturbative quark propagator provide evidence that centre vortices underpin dynamical chiral symmetry breaking [21], and the removal of centre vortices from the gluon fields restores chiral symmetry [22]. Centre vortices are the seeds of dynamical chiral symmetry breaking.

In light of the importance of these most fundamental aspects of QCD vacuum structure, visualisations of the complex structures formed by the projected centre vortices in SU(3) gauge theory have been presented in Ref. [23]. Here we explore their correlation with the topological charge density of the gluon fields and present a new animation [24, 25] showcasing a prevalence of branching points in the flow of centre charge that look like monopole or anti-monopole contributions. Details of the identification of projected centre vortices and the techniques used to render them are

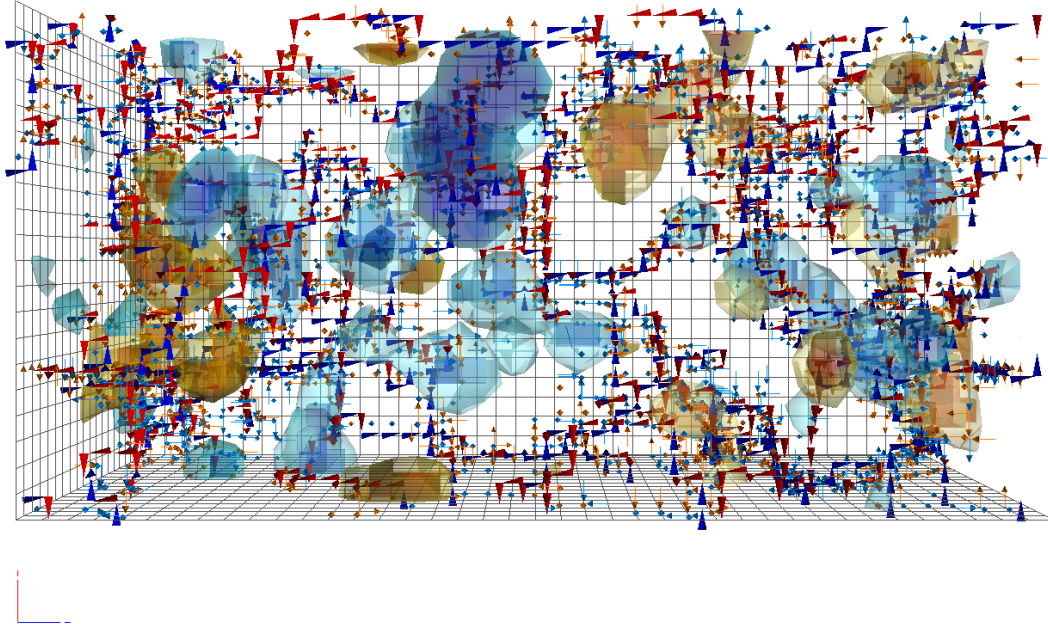


Figure 3: The projected centre-vortex structure of the gluon field. The flow of centre charge is illustrated by the red and blue jets. The motion of the jets through time-oriented plaquettes is indicated by the orange and cyan arrows. The correlation of the vortex lines with the topological charge density is examined by volume-rendering the topological charge density in a translucent manner. Additional details are available in Ref. [23]. (Click on the image to activate it in Adobe Reader. Click and drag to rotate, Ctrl-click to translate, Shift-click or mouse wheel to zoom. Right click to access the “Views” menu.)

described in Ref. [23] of these proceedings. The topological charge is determined using the techniques of Sec. 2 with eight sweeps of $\mathcal{O}(a^4)$ -three-loop improved cooling [11].

The structure of projected centre vortices and their correlation with the topological charge density is illustrated¹ in Fig. 3. Inspection of the vortices reveals the flow of centre charge, intersection points and a prevalence of branching points that look like monopole or anti-monopole contributions. An engaging presentation suitable for outreach activities is presented in the animation of Ref. [24] with the original HD-streaming animation available via Ref. [25].

5. Interplay of QED and QCD in the Nontrivial Vacuum

The QCDSF collaboration have generated gauge field configurations incorporating the dynamical effects of both QCD and QED [26, 27]. As the dynamics of the QCD fields include the creation of quark-antiquark pairs, their electric charge – enhanced by a factor of 10 in the simulations – participates in a dynamical manner through QED interactions. Here we consider the $24^3 \times 48$ lattice

¹To interact with Fig. 3, open this pdf document in Adobe Reader 9 or later. Linux users should install [Adobe acroread version 9.4.1](#), the last edition to have full 3D support. From the “Edit” menu, select “Preferences...” and ensure “3D & Multimedia” is enabled and “Enable double-sided rendering” is selected.

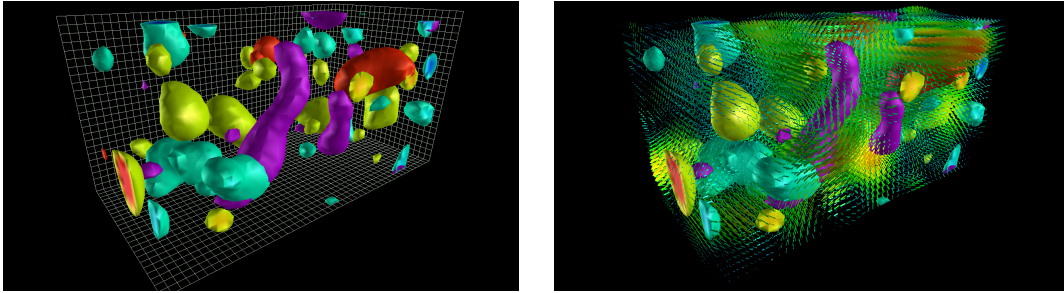


Figure 4: Frames from the animation of Refs. [28, 29] illustrating the topological charge density of QCD and the electric charge density of QED (left) with the QED magnetic field superposed (right). Regions of significant topological charge density are rendered in red through yellow (blue through cyan) for positive (negative) values of the density. Regions of large electric charge density are rendered in red (purple) for positive (negative) charge and the associated magnetic field is illustrated by the vector field.

at the flavor-symmetric point with a lattice spacing of 0.068 fm [26]. The calculations of the fields proceed in a manner analogous to that presented in Sec. 2.

There is an interesting relationship between the electric charge density, obtained through the divergence of the electric field, and the topological charge density of QCD. As the electric charge moves, magnetic fields are created in the vacuum. The movement of electric charge relative to the magnetic field, particularly when that charge is influenced by the topological charge density of QCD is of particular interest. Figure 4 presents two frames from the animation of Refs. [28, 29]. In this animation the topological charge density is compared with the electric charge density of quark-antiquark pairs and the magnetic field they create.

References

- [1] D. B. Leinweber, *Visual QCD Archive*, 2002.
<http://www.physics.adelaide.edu.au/theory/staff/leinweber/VisualQCD/QCDvacuum/>.
- [2] D. Leinweber, *QCD Lava Lamp*, 2004.
<http://www.physics.adelaide.edu.au/theory/staff/leinweber/VisualQCD/QCDvacuum/su3b600s24t36cool30action.gif>.
- [3] F. Wilczek, *2004 Nobel Prize Lecture*, 2004.
<https://www.nobelprize.org/prizes/physics/2004/wilczek/lecture/>.
- [4] D. B. Leinweber, *Visualizations of Quantum Chromodynamics*, 2004.
<http://www.physics.adelaide.edu.au/theory/staff/leinweber/VisualQCD/Nobel/>.
- [5] D. Muller, *Empty Space is NOT Empty*, 2013. <https://www.youtube.com/watch?v=S1tFT4smd6E>.
- [6] D. Muller, *Your Mass is NOT From the Higgs Boson*, 2013.
<https://www.youtube.com/watch?v=Ztc6QPNUqls>.
- [7] D. B. Leinweber, *Origin of Mass*, 2008.
<http://www.physics.adelaide.edu.au/theory/staff/leinweber/VisualQCD/OriginMass/>.
- [8] D. B. Leinweber and E. Puckridge, *Structure of the QCD Vacuum*, 2019.
<https://youtu.be/WZgZI5vymiM>.
- [9] D. B. Leinweber and E. Puckridge, *Structure of the QCD Vacuum*, 2018.
<http://www.physics.adelaide.edu.au/cssm/lattice/QCDvacuum/ChromoElectroMagneticFields.mp4>.

- [10] S. O. Bilson-Thompson, D. B. Leinweber, and A. G. Williams, *Highly improved lattice field strength tensor*, *Annals Phys.* **304** (2003) 1–21, [[hep-lat/0203008](#)].
- [11] S. O. Bilson-Thompson, D. B. Leinweber, A. G. Williams, and G. V. Dunne, *Comparison of $|Q| = 1$ and $|Q| = 2$ gauge-field configurations on the lattice four-torus*, *Annals Phys.* **311** (2004) 267–287, [[hep-lat/0306010](#)].
- [12] F. D. R. Bonnet, P. O. Bowman, D. B. Leinweber, A. G. Williams, and D. G. Richards, *Discretization errors in Landau gauge on the lattice*, *Austral. J. Phys.* **52** (1999) 939–948, [[hep-lat/9905006](#)].
- [13] F. M. Stokes, W. Kamleh, and D. B. Leinweber, *Visualizations of coherent center domains in local Polyakov loops*, *Annals Phys.* **348** (2014) 341–361, [[arXiv:1312.0991](#)].
- [14] C. Gattringer and A. Schmidt, *Center clusters in the Yang-Mills vacuum*, *JHEP* **01** (2011) 051, [[arXiv:1011.2329](#)].
- [15] F. M. Stokes, W. Kamleh, and D. B. Leinweber, *Centre Domains in the QCD Vacuum - Smeared Phase*, 2014. <https://youtu.be/KkiOQOOB69k>.
- [16] F. M. Stokes, W. Kamleh, and D. B. Leinweber, *Centre Domains in the QCD Vacuum - Smeared Phase*, 2014. <http://www.physics.adelaide.edu.au/cssm/lattice/centreclusters/smeared-phase.mp4>.
- [17] F. M. Stokes, W. Kamleh, and D. B. Leinweber, *Centre Domains in the QCD Vacuum - Smeared Magnitude*, 2014. <https://youtu.be/T4sRON6uOz0>.
- [18] F. M. Stokes, W. Kamleh, and D. B. Leinweber, *Centre Domains in the QCD Vacuum - Smeared Magnitude*, <http://www.physics.adelaide.edu.au/cssm/lattice/centreclusters/smeared-magnitude.mp4>.
- [19] K. Langfeld, *Vortex structures in pure $SU(3)$ lattice gauge theory*, *Phys. Rev.* **D69** (2004) 014503, [[hep-lat/0307030](#)].
- [20] J. C. Biddle, W. Kamleh, and D. B. Leinweber, *Gluon propagator on a centre-vortex background*, [arXiv:1806.0430](#).
- [21] D. Trewartha, W. Kamleh, and D. Leinweber, *Evidence that centre vortices underpin dynamical chiral symmetry breaking in $SU(3)$ gauge theory*, *Phys. Lett.* **B747** (2015) 373–377, [[arXiv:1502.0675](#)].
- [22] D. Trewartha, W. Kamleh, and D. Leinweber, *Centre vortex removal restores chiral symmetry*, *J. Phys.* **G44** (2017), no. 12 125002, [[arXiv:1708.0678](#)].
- [23] J. C. Biddle, W. Kamleh, and D. B. Leinweber, *Visualizations of Centre Vortex Structure in Lattice Simulations*, *PoS LATTICE2018* (2018) 256.
- [24] J. Biddle, W. Kamleh, D. Leinweber, and H. Piercy, *Centre Vortices in the Gluon Field of the QCD Vacuum*, 2019. <https://youtu.be/CDdmx989quA>.
- [25] J. Biddle, W. Kamleh, D. Leinweber, and H. Piercy, *Centre Vortices in the Gluon Field of the QCD Vacuum*, 2018. <http://www.physics.adelaide.edu.au/cssm/lattice/QCDvacuum/CentreVorticesTopQ.mp4>.
- [26] R. Horsley et al., *Isospin splittings of meson and baryon masses from three-flavor lattice QCD + QED*, *J. Phys.* **G43** (2016), no. 10 10LT02, [[arXiv:1508.0640](#)].
- [27] R. Horsley et al., *QED effects in the pseudoscalar meson sector*, *JHEP* **04** (2016) 093, [[arXiv:1509.0079](#)].
- [28] J. Charvetto, W. Kamleh, D. Leinweber, R. Young, and J. Zanotti, *Interplay of Quantum Electrodynamics and Quantum Chromodynamics in the Nontrivial Vacuum*, 2019. <https://youtu.be/9TJe1Pr5c9Q>.
- [29] J. Charvetto, W. Kamleh, D. Leinweber, R. Young, and J. Zanotti, *Interplay of Quantum Electrodynamics and Quantum Chromodynamics in the Nontrivial Vacuum*, 2018. <http://www.physics.adelaide.edu.au/cssm/lattice/QEDnQCD/QEDnQCDvacuum.mp4>.